Available online at www.sciencedirect.com
SciVerse ScienceDirect
Geochimica et Cosmochimica Acta xxx (2013) xxx–xxx
Geochimica et Cosmochimica Acta
www.elsevier.com/locate/gca

Seasonal cycles in radium and barium within a subterranean estuary: Implications for groundwater derived chemical fluxes to surface waters

Meagan Eagle Gonneea[a,*], Ann E. Mulligan[b], Matthew A. Charette[a]

[a] Department of Marine Chemistry and Geochemistry, Woods Hole Oceanographic Institution, 266 Woods Hole Road, MS 25, Woods Hole, MA 02543, United States

[b] Marine Policy Center, Woods Hole Oceanographic Institution, 266 Woods Hole Road, MS 25, Woods Hole, MA 02543, United States

Received 27 January 2012; accepted in revised form 27 May 2013; available online xxxx

Abstract

There is increasing evidence that submarine groundwater discharge (SGD) is an important source of water and dissolved materials to the ocean. One of the primary tracers of this process is the quartet of radium isotopes (^{223}Ra, ^{224}Ra, ^{226}Ra and ^{228}Ra), whereby excess activities in surface waters can often be attributed to an input supplied via SGD. This approach requires the radium end member activity to be well constrained, however, natural variability in groundwater radium may span several orders of magnitude. Therefore, this variability is usually the main driver of uncertainties in volumetric SGD estimates. To investigate the physical and biogeochemical controls on groundwater radium activities, we conducted a three-year time series of radium and barium, a chemical analogue for radium, within the subterranean estuary of a coastal aquifer (Waquoit Bay, MA, USA). Gonneea et al. (2013) demonstrated that movement of the salinity interface within the subterranean estuary is driven by changes in the hydraulic gradient between groundwater level and sea level height. For Waquoit Bay, seasonal scale sea level change, not groundwater level, was the main driver in hydraulic gradient fluctuations. Seasonal changes in groundwater chemistry can be attributed to the resulting movement of the salinity transition zone between terrestrial and marine groundwater. Landward movement of the interface results in a large release of radium isotopes (^{226}Ra = 1400 dpm 100 L^{-1}) and barium (3000 nmol kg^{-1}) associated with an increase in groundwater salinity. The magnitude of these releases cannot be explained by *in situ* production or weathering alone, but is likely due to salinity driven desorption from surface-bound sediment inventory. The timing of these peak concentrations is not always in phase with model-derived estimates of SGD; as a result, the groundwater concentration rather than the water flux is the main driver of Ra and Ba inputs to Waquoit Bay surface waters. The behavior of the subterranean estuary as an ion exchange reservoir has important implications for the timing and flux of various nutrients and pollutants that transit this region prior to discharge. In addition to modulating chemical fluxes via submarine groundwater discharge on seasonal time scales, transgression of the subterranean estuary may alter the input of chemicals to the ocean on decadal and longer time scales. During this study, the observed excess flux of ^{226}Ra and Ba from the subterranean estuary can be accounted for with sorbed sediment pools and accelerating rates of sea level rise in this region.

1. INTRODUCTION

Groundwater discharge at the land–ocean interface is driven by a variety of physical processes (Robinson et al., 2006; Mulligan and Charette, 2009; Michael et al., 2011). Fresh, terrestrially-derived groundwater flows to the coast,

Abbreviations: SGD, submarine groundwater discharge; STE, sub terranean estuary; STZ, salinity transition zone.

* Corresponding author. Tel.: +1 508 289 3236.
E-mail addresses: mgonneea@whoi.edu (M.E. Gonneea), amulligan@whoi.edu (A.E. Mulligan), mcharette@whoi.edu (M.A. Charette).

0016-7037/$ - see front matter © 2013 Published by Elsevier Ltd.
http://dx.doi.org/10.1016/j.gca.2013.05.034

where it mixes with seawater that has inundated the coastal aquifer (marine groundwater), resulting in a deep circulation cell that rises along the density stratified salinity transition zone (STZ) and discharges to surface waters (Moore, 1999; Michael et al., 2005; Charette, 2007). In addition, short temporal period tidal and wave pumping result in seawater exchange at the sediment–water interface of the subterranean estuary (Robinson et al., 2006; Li et al., 2009; Xin et al., 2010; Abarca et al., 2013).

Water discharging across the ocean–aquifer boundary has a unique 2chemistry since it is a complex mixture of terrestrial and marine groundwater that has experienced a range of different residence times within the subterranean estuary (STE), the below ground analogue to surface estuaries with similarly dynamic salinity and chemical gradients (Moore, 1999). Trace metal and radionuclide cycling within subterranean estuaries is expected to have a large influence on total chemical flux discharging via submarine groundwater discharge (SGD). Much of our knowledge of chemical cycling within this zone is derived from studies based on single time points, with little known about the time scale or magnitude of temporal variability (Bone et al., 2006; Charette and Sholkovitz, 2006; Paytan et al., 2006; Windom et al., 2006; Beck et al., 2007; Perry et al., 2009; Beck et al., 2010; Santos et al., 2011). Recently Gonneea et al. (2013) showed that seasonal-scale variability in the coastal hydraulic gradient results in dynamic movement of the STZ and corresponding changes in the chemical environment of the subterranean estuary.

Such seasonal variability is particularly relevant to radioisotopic tracers that have extended our capability to quantify SGD (Moore, 2003). These tracers, which include the radium quartet (^{223}Ra $t_{1/2} = 3.66$ d, ^{224}Ra $t_{1/2} = 11.4$ d, ^{228}Ra $t_{1/2} = 5.75$ y and ^{226}Ra $t_{1/2} = 1{,}600$ y), are enriched in groundwater, up to several orders of magnitude above ambient seawater, and upon discharge to coastal waters their activity is a function only of mixing and decay. However, to refine the utility of radium isotopes as SGD tracers, it is necessary to understand their geochemical cycling within the subterranean estuary. Indeed, estimates of SGD based on radium tracers can only be resolved to the level that groundwater end member radium activities can be constrained, and variability in groundwater radium activity remains the largest source of uncertainty in radium tracer based SGD calculations (Charette, 2007; Ferrarin et al., 2008; Moore et al., 2008; Breier et al., 2010). Several studies to date have identified a seasonal aspect to SGD based on seasonal changes in radium inventories of surface waters (Kelly and Moran, 2002; Hougham et al., 2008; Breier et al., 2010). Seasonal cycles in surface water radium inventories may result either from a change in water flux with no concurrent change in the groundwater end member activity, from a steady water flux and dynamic groundwater end member, or some combination of the two. Thus, it is imperative to understand radium cycling within the STE to make accurate estimates of groundwater discharge based on radium tracers.

Most previous research on radium cycling within aquifers has focused predominantly on inland aquifers without dynamic mixing zones (Tricca et al., 2001; Ku et al., 2009). In these aquifers, the dominant source of radium is via *in situ* production from uranium and thorium parents (Porcelli, 2008). This is ultimately true of coastal groundwater systems as well, however, the large inventory of radium observed within coastal groundwater, particularly for the long-lived isotopes ^{226}Ra and ^{228}Ra, cannot be supported only by decay and recoil from aquifer sediments immediately at the coast (Rama and Moore, 1996). Indeed, modeling studies that have attempted to evaluate Ra cycling within the STE have demonstrated that even relatively simple one-dimensional advective transport models are underconstrained in terms of the chemical processes affecting Ra distribution, particularly for the longer lived isotopes (Krest and Harvey, 2003; Michael et al., 2011; Kiro et al., 2012). This is due in part to the main factors that influence radium partitioning between the dissolved and solid phases (see recent review by Beck and Cochran, 2013). The salinity of groundwater has long been recognized as a major influence on the radium partition coefficient (Elsinger and Moore, 1980; Webster et al., 1995; Gonneea et al., 2008). In addition, the presence of Mn–Fe oxides has been shown to increase radium adsorption both in laboratory experiments (Moore and Reid, 1973; Koulouris, 1996; Beck and Cochran, 2013) and for *in situ* aquifer sediments (Gonneea et al., 2008). Recent work by Beck and Cochran (2013) suggests groundwater pH may potentially exert a similar magnitude control on radium partitioning within the subterranean estuary as groundwater salinity. To gain insight into the mechanisms that control both temporal variability and the large and sustained flux of radium isotopes from coastal aquifers, we evaluate both radium and barium (Ba) cycling within the STE across a three-year time series of groundwater chemistry. Ba serves as a chemical analogue to Ra in terms of sorption and redox chemistry, yet is not influenced by radioactive production/decay processes.

Within the Waquoit Bay subterranean estuary the dynamic seasonal movement of the STZ responds to oscillations in the aquifer hydraulic gradient that are dominated by seasonal scale sea level variability (Gonneea et al., 2013). Sediments within the mixing zone are alternately inundated with terrestrial and marine groundwater over the course of a year. This study explores the chemical cycling induced by these seasonal changes. Here we present the first monthly time series measurements of radium and barium within a permeable sand subterranean estuary. We will evaluate the relative importance of the geochemical controls known to affect radium cycling within the Waquoit Bay STE on seasonal time scales. Finally, to place the chemical cycling of Ra and Ba within the STE in the context of chemical fluxes via SGD, we use model derived groundwater fluxes and salinity to calculate total fluxes of Ra and Ba via SGD on the same monthly resolution as the groundwater time series.

2. METHODS

2.1. Field site

Waquoit Bay is a shallow estuary on the southern shore of Cape Cod, MA (Fig. 1). In this region, surface geology is

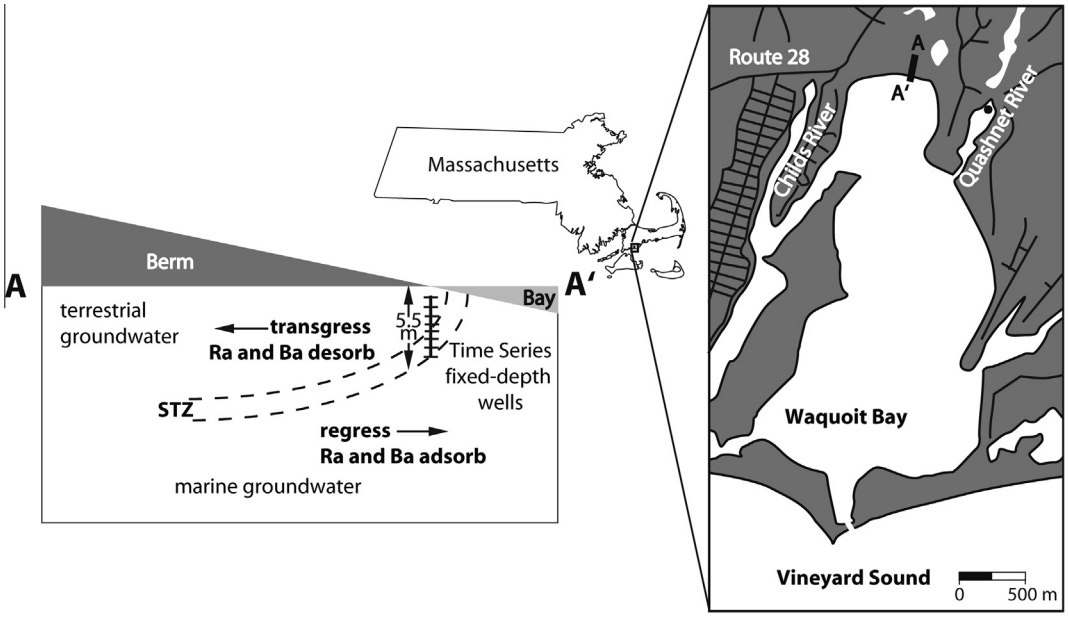

Fig. 1. Waquoit Bay, MA, USA. The time series wells were installed within the mixing zone of the subterranean estuary and sampled monthly during the three-year time series. STZ is the salinity transition zone where mixing between terrestrial and marine groundwater occurs. The STZ moves in response to the hydraulic gradient across the subterranean estuary. During periods of high hydraulic gradient (generally low sea level), the salinity interface moves seaward and Ra and Ba adsorb onto sediments, while during low hydraulic gradient, the interface moves landward, causing release of these elements.

dominated by sand and gravel glacial outwash plains formed during the last glaciation ~14,000 years ago. The upper 10 m of the Cape Cod aquifer, where the Waquoit Bay subterranean estuary is located, consists of fairly homogenous permeable sediments (Cambareri and Eichner, 1998). Boreholes drilled through the STE of Waquoit Bay reveal fine to coarse sand (0–10 m) underlain by fine to very fine sand and silt (Cambareri and Eichner, 1998). Grain size analysis of three sediment cores from the top 8 m within the STE indicates that the shallow sediment has a grain size range from 450 to 650 microns with no vertical structure apparent (Charette, unpublished data). The primary sand grains are quartz, with <1% of plagioclase along with traces of clinopyroxene, amphibole, white mica, magnetite and at least one other oxide (goethite or hematite) (Charette et al., 2005). Polymineralic fragments in the sands probably represent granite, schist, amphibolite and gabbro. Within the Waquoit Bay subterranean estuary, there are well-defined regions of Fe-oxides (Charette et al., 2005) and Mn-oxides that have been shown to sorb radium (Dulaiova et al., 2008; Gonneea et al., 2008).

These highly permeable sediments result in high groundwater recharge, with about half of precipitation becoming recharge (Cambareri and Eichner, 1998). Precipitation averaged 126 cm y^{-1} from 2004 to 2007 with no clear seasonal cycle in rainfall (may be accessed at http://cis.whoi.edu/science/PO/climate/index.cfm). Since rates of evapotranspiration peak in summer months, the greatest potential for groundwater recharge occurs during the winter and spring (Michael et al., 2003). Waquoit Bay experiences diurnal tides with an average tidal range of 1.2 m. At the head of Waquoit Bay there is a well-defined subterranean estuary with a salinity transition zone that occurs over a narrow region (~1 m thick (Charette et al., 2005)). The salinity interface moves on seasonal time scales, which results in a variety of chemical processes, including ion exchange (adsorption/desorption reactions) and redox cycling (Charette and Sholkovitz, 2006; Gonneea et al., 2008; Abarca et al., 2013; Beck and Cochran, 2013). Terrestrial groundwater discharge accounts for approximately 80% of the flow through the subterranean estuary at the head of the bay (Mulligan and Charette, 2006). Further out in the bay (>100 m from mean sea level), where tidal and wave pumping dominate, the discharge consists of recirculated seawater. SGD from this location is not considered here since it does not transit the subterranean estuary and is unlikely to be an important flux term for the long-lived radium isotopes (Michael et al., 2011).

2.2. Field methods

A series of AMS™ Dedicated Gas Vapor Probe Tips were installed with an AMS™ Retract-a-Tip probe system modified for long-term installation at the head of Waquoit Bay within the subterranean estuary in October 2004 (Fig. 1, Charette and Allen (2006)). When the metal walls of the piezometer are withdrawn from the ground, a stainless steel well point attached to ¼ inch nylon tubing remains. The well points, each with a screened interval of 2.5 cm, were installed at eight depths below the beach surface across the subterranean estuary ranging from 2.4 to 5.4 m. Samples were collected every month from October 2004 to October 2007 during the same tidal cycle and phase (four hours past high tide, ~3 days before the monthly

spring tide) to reduce the potential variability associated with tidal fluctuations, although the salinity mixing zone discussed here does not respond on tidal time scales (Gonneea et al., 2013). Dissolved oxygen, pH, Eh and salinity were measured with a YSI™ sonde after pumping approximately 1 L (6–13 well volumes, flow rate approximately 200 ml min^{-1}). Samples were then collected for salinity, trace metals, and radium isotopes (4 L). Salinity, pH, Eh and dissolved oxygen were stable throughout the sampling, as verified by YSI™ readings, thus we assume that water was being extracted from the same density horizon, and not across density gradients (i.e. not from different depths at this fixed location).

A sediment core down to 7 m was collected in June 2006 from the region of the groundwater time series. Collection and geochemical analysis of this core has been described previously and is presented here to aid interpretation of groundwater geochemical cycling (Dulaiova et al., 2008; Gonneea et al., 2008). All sediment trace metal data is for the fraction associated with amorphous and crystalline oxides, as defined by a hydroxylamine hydrochloride and acetic acid chemical leach, with the exception of ion exchangeable, organic and oxide associated fractions used to calculate sediment inventory (Hall et al., 1996). All radionuclide data is for the whole sediment, with the exception of the adsorbed ^{226}Ra values used to calculate sediment inventory (Dulaiova et al., 2008; Gonneea et al., 2008).

2.3. Laboratory methods

Radium isotopes were extracted with Mn fibers, rinsed with Ra-free water to remove salts that interfere with counting (Sun and Torgersen, 1998), partially dried and placed within a delayed coincidence counter to measure ^{224}Ra and ^{223}Ra (Moore and Arnold, 1996). The fibers were counted at four weeks to correct for ^{228}Th supported ^{224}Ra on the fibers. Samples were then ashed (820 °C, 16 h), homogenized and capped with epoxy, prior to being placed within a well-type gamma spectrometer to measure ^{226}Ra (via ^{214}Pb at 351.9 keV) and ^{228}Ra (via ^{228}Ac at 911 keV) (Charette et al., 2001). All detectors were standardized using a NIST-certified Standard Reference Material sorbed to Mn fibers and prepared in the same manner as the samples. Detection limits calculated with the Currie Hypothesis test for these samples were 0.2 dpm (5 dpm/100 L for 4 L groundwater samples) (De Geer, 2004). ^{224}Ra and ^{228}Ra activities were decay corrected to the time of collection. ^{223}Ra activities were at or near detection for a significant portion of the time series so are not reported here. Sediment ^{226}Ra (via ^{214}Pb at 351.9 keV), ^{228}Ra (via ^{228}Ac at 338 keV) and ^{224}Ra (via ^{212}Pb at 238 keV) activities were measured on planar-type gamma spectrometers after aging epoxied samples for at least 3 weeks to ensure secular equilibrium between ^{226}Ra and its daughter radionuclides. The program GESPECOR, a Monte Carlo based software used for calibration of pure Ge detectors, was used to calibrate the detector.

Salinity was measured with a Guideline AutoSal instrument. Groundwater concentrations of dissolved Mn, Fe and Ba were analyzed via inductively coupled mass spectrometry on a Finnigan Element II high resolution ICP-MS at Woods Hole Oceanographic Institution. Each sample was diluted 1:20 with 1 N Optima nitric acid. Indium (In) was used as an internal standard to account for instrument drift and matrix effects of the solution. Count rates for all elements were normalized to In measured in samples and standards.

2.4. Hydrology model

Groundwater flux through the STE at Waquoit Bay was evaluated with a simulation model of groundwater flow and salt transport using the USGS code SEAWAT (Mulligan et al., 2011). The model was used to represent conditions at Waquoit Bay but was not calibrated to field data, hence results are considered approximate and largely qualitative. However, model sensitivity was sufficient to evaluate the importance of water flux versus groundwater concentration on radium and barium chemical fluxes via submarine groundwater discharge.

Briefly, the simulation model is a two-dimensional cross section of a homogeneous unconfined aquifer below a sloping beach (0.08 m/m). The simulated domain measures 130 m long and 10 m deep. Flow boundary conditions include variable head along the upland margin and seaward edge, with no flow across the bottom of the domain and no recharge across the top boundary. The upland boundary is coincident with the location of an observation well, CCC1, which was monitored at 15-min intervals during most of the geochemical sampling (Gonneea et al., 2013). Monthly average groundwater levels at this well were specified as the upland boundary. The marine boundary was specified as the monthly average sea level from the NOAA Woods Hole tidal gauge (available at http://tidesandcurrents.noaa.gov/station_info.shtml?stn=8447930%20Woods%20Hole,%20MA) for the period from January 2005 to May 2007. No sea level data from Waquoit Bay exist for the duration of the field campaign and so the Woods Hole gauge is used as a surrogate. Linear interpolation between monthly groundwater levels and sea level data points was used to estimate boundary conditions at 15-day intervals to coincide with the stress periods used in the model. Within each 15-day stress period, tidal and upland boundary conditions remain constant but these values can vary from one stress period to the next. Simulations were run for the equivalent of 2.3 y (January 2005 to May 2007), the length of time data were available to define the upland boundary condition. Model-derived SGD results were averaged over 30 days to coincide with the time series chemical data and binned into five different groups based on the salinity of the discharging water. Additional details of the domain and SEAWAT-specific model parameters can be found in Mulligan et al. (2011).

3. RESULTS

The time series offers a window into the chemistry of the subterranean estuary at a fixed point over 3 y. When plotted as a time series, with time on the *x*-axis, movement of the salinity transition zone appears as a vertical oscillation

Please cite this article in press as: Gonneea M. E., et al. Seasonal cycles in radium and barium within a subterranean estuary: Implications for groundwater derived chemical fluxes to surface waters. *Geochim. Cosmochim. Acta* (2013), http://dx.doi.org/10.1016/j.gca.2013.05.034

between periods of high and low salinity at this fixed location. Results from the three-year time series are presented in contour plots in Fig. 2 to highlight the seasonal oscillations in the various parameters, in box and whisker plots in Fig. 3 to demonstrate the depth dependence and the total variability observed in the parameters and as element versus salinity and pH to reveal trends sensitive to those parameters in Fig. 4.

3.1. Salinity transition zone

The salinity of the subterranean estuary oscillated throughout the three-year time series and ranged from 0 to 28 (Fig. 2a). At this location within the STE, the depth range that experienced the largest salinity excursions from a baseline low salinity was 3.1–4.1 m (Fig. 3a). At this depth, the salinity was below 2 at least 50% of the time. Above this, the STE was dominated by terrestrial groundwater throughout the measurement period, while below 4.1 m, the salinity increased with depth, indicating the increasing dominance of marine groundwater. Salinity excursions within the upper fresh portion of the STE were observed periodically throughout the time series (November 2004, October 2005, February 2006 and June 2007) and likely resulted from infiltration of bay water during a high tide and subsequent density driven mixing into the upper STE. In addition, during February 2006, the entire STE was dominated by terrestrial groundwater, possibly due to the sustained high hydraulic gradient from December 2005 to March 2006 (Gonneea et al., 2013). Salinity maximums occurred throughout the entire vertical section of the STE in October 2004, June–December 2005, May 2006, August–November 2006 and August 2007. pH does not show as pronounced seasonal variability as salinity. pH is generally 7–8 in the deep marine groundwater, and lower (5–6) in the terrestrial groundwater and mixing zone (Fig. 2b). The region above 4.1 m tends to have the largest dynamic range in pH (Fig. 3b).

3.2. Trace metals and radium

Groundwater Ra activities fluctuated in concert with the salinity changes in the STE. ^{226}Ra ranged from below detection (5 dpm 100 L^{-1}, with approximately 20% of the time series radium samples below detection, mostly terrestrial groundwater samples) to 1400 dpm 100 L^{-1} (Fig. 2b). Estuarine release at intermediate salinities is apparent, with peak activities around salinity 15 (Fig. 4c). A radium sorption edge is apparent, with no ^{226}Ra activity >200 dpm 100 L^{-1} above pH 6, indicating that pH is a potential control on radium activities within the STE (Fig. 4d). Activities within the marine groundwater were relatively constant at 30 to 130 dpm 100 L^{-1}, while the largest releases were observed in the sediment from 3.1 to 4.1 m that was inundated by terrestrial groundwater at least 50% of the time (Fig. 3c). Groundwater ^{224}Ra and ^{228}Ra displayed similar seasonal oscillations and activity extremes, from detection to maximum activities of 11,600 and 5300 dpm 100 L^{-1}, respectively (Supplementary Figs. 1 and 2). Total sediment radium showed little variation with depth and averaged 370 ±

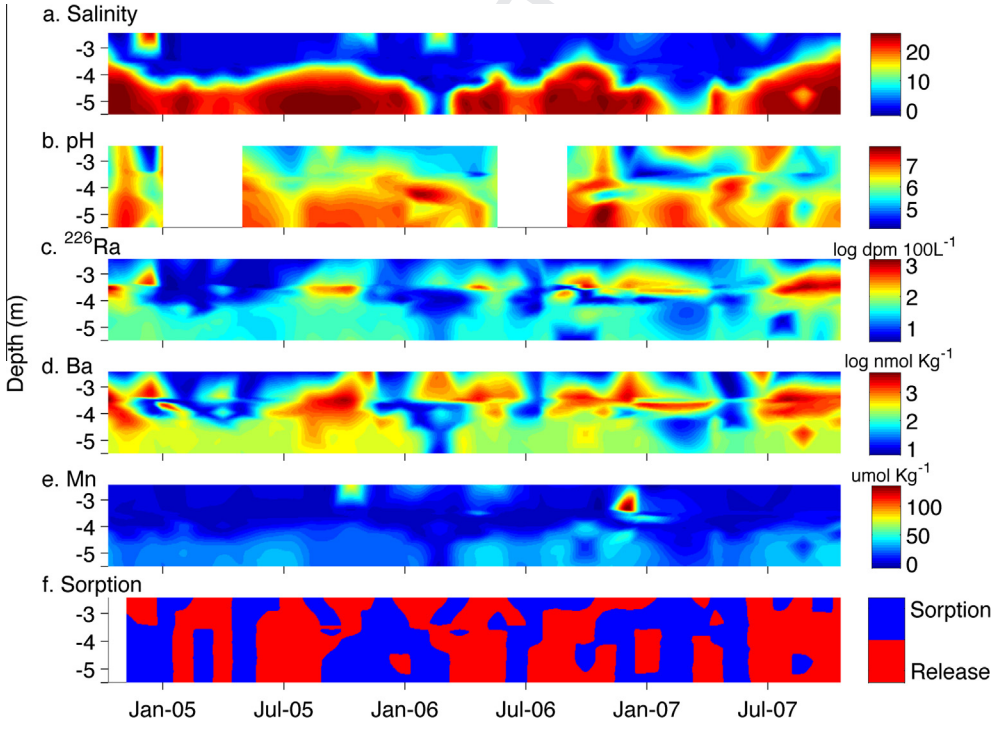

Fig. 2. Time series data from October 2004 to October 2007 for (a) salinity, (b) pH, (c) dissolved ^{226}Ra, (d) dissolved barium and (e) dissolved manganese. Also shown (f) is the sorption potential, as determined by the change in salinity from time point $t_{n+1} - t_n$. Note the log scale in (b) and (c). Data were contoured in Matlab using a cubic interpolation.

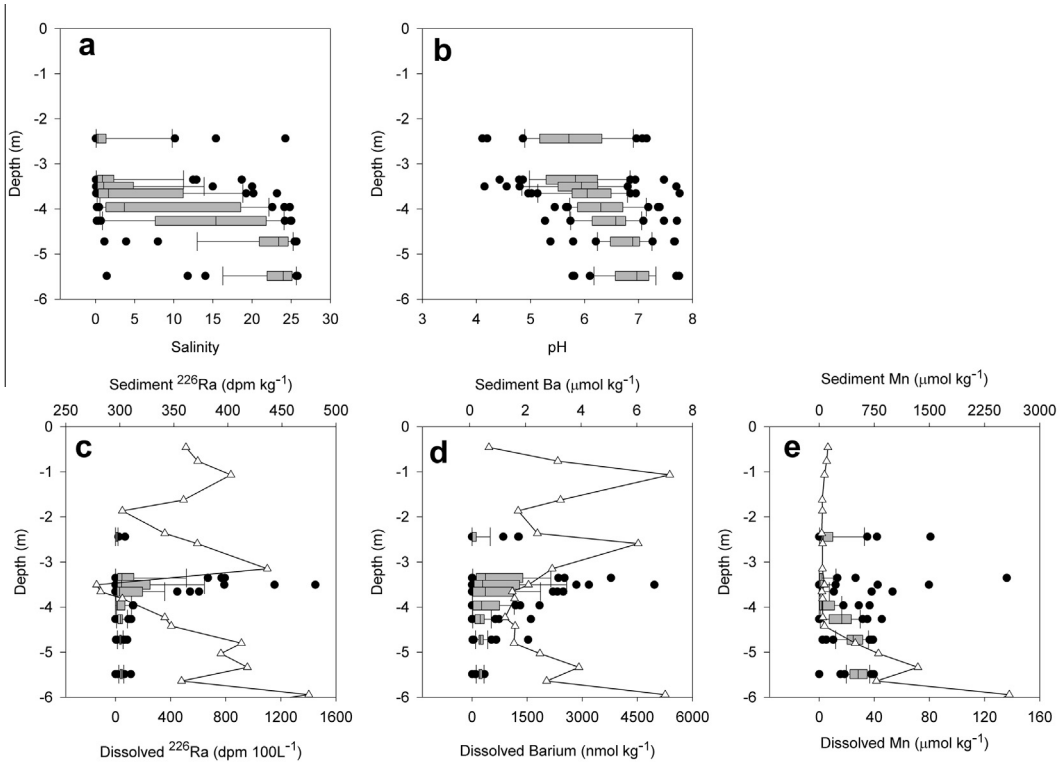

Fig. 3. Box and whisker plots of (a) salinity, (b) pH, (c) dissolved and sediment surface oxide associated Mn, (d) dissolved and total sediment ^{226}Ra and (e) dissolved and sediment surface oxide associated Ba. These plots contain all data points over the three-year time series for each depth. The gray box marks the 25th, 50th and 75th percentile of samples, with the 5th and 95th percentile of samples marked by the lines extending from the box. Outliers are plotted as points. The sediment profiles were collected in June 2006 and are shown here to provide sediment geochemical background for interpreting the time series water chemistry (Gonneea et al., 2008).

60 dpm kg^{-1} for ^{226}Ra, 410 ± 90 dpm kg^{-1} for ^{228}Ra, and 700 ± 160 dpm kg^{-1} for ^{224}Ra (supported by ^{228}Th). We assume that ^{224}Ra is in secular equilibrium with ^{228}Th since sediments were aged at least three weeks prior to counting.

Like its alkaline earth counterpart (Ra), dissolved Ba concentrations also oscillated with the movement of the STZ from less than 10 to greater than 3,000 nmol kg^{-1} (Fig. 2c). The greatest Ba increase occurred during high salinity periods in the band of sediments from 3.1 to 4.1 m. Dissolved Ba was relatively constant (100–400 nmol kg^{-1}) in the high salinity portion of the STE (Fig. 3d). As with ^{226}Ra, peak concentrations of Ba are observed around salinity 15 (Fig. 4a). However, estuarine release is apparent from a salinity of ~2.

Oscillations between high and low concentrations were observed in the dissolved Mn and Fe records (Fig. 2d and Supplemental Fig. 1). Dissolved Mn tracked the increase in salinity as the salinity transition zone moved landward and seaward. Note however that the dissolved Mn was high (30 μmol kg^{-1}) only within the core of the high salinity zone (depth >4 m), a region that was marked by sediments coated with Mn-oxides (Figs. 3b and 4e). Above this region, there were minimal fluctuations in dissolved Mn with a few large excursions (80–140 μmol kg^{-1}) above the relatively constant <1 μmol kg^{-1} background (Fig. 4e). Dissolved Fe was also quite low, at or below detection (0.1 μmol kg^{-1}) for the majority of the time series. Dissolved Fe increased to 20–80 μmol kg^{-1} several times at shallow depths, coincident with the first occurrence of surface adsorbed Fe-oxides on the sediment (Supplemental Fig. 2).

4. DISCUSSION

4.1. Periodic release of radium and barium via ion exchange

Large releases of radium and barium into the groundwater were observed in the subterranean estuary of Waquoit Bay and corresponded to fluctuations in salinity. The salinity of the STE at the time series location fluctuated as the salinity transition zone moved in response to changes in the hydraulic gradient (Gonneea et al., 2013). Periods dominated by marine groundwater corresponded to low hydraulic gradients and landward movement of the STZ, while increases in the hydraulic gradient resulted in seaward movement of the STZ and freshening at the time series location. The radium and barium partition coefficients (K_d, the ratio of adsorbed to dissolved species) are a function of salinity, such that low salinity periods favor the adsorbed phase, while an increase in salinity results in a greater dissolved fraction (in these sediments *in situ* Ra $K_d \approx 1000$ (L/kg) at salinity 0 and $K_d \approx 90$ (L/kg) at salinity 20 (Gonneea et al., 2008) and Ba $K_d \approx 1000$ (L/kg) for glacial/fluvial material (Grutter et al., 1992)). In addition, K_d may be in-

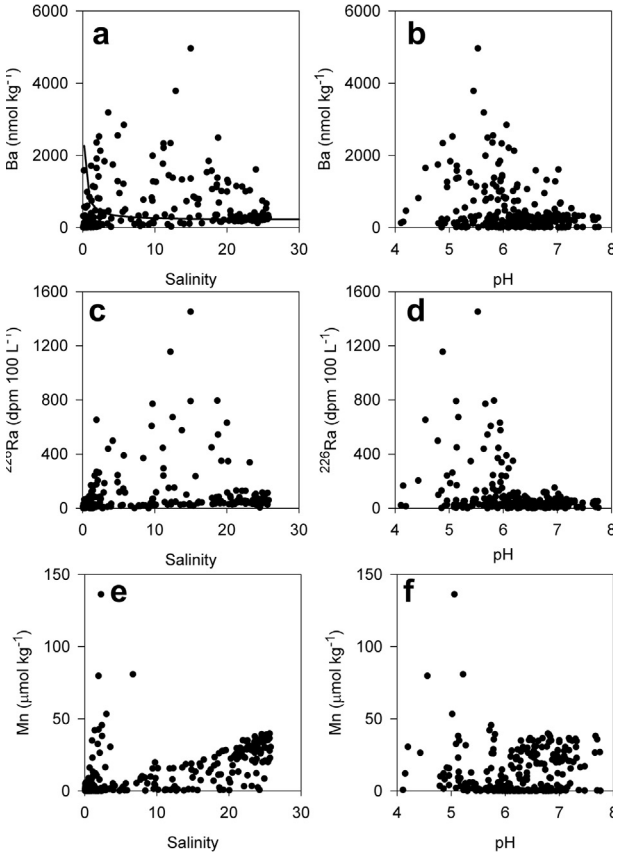

Fig. 4. Element versus salinity plots for (a) Ba, (c) ^{226}Ra and (e) Mn and element versus pH plots for (b) Ba, (d) ^{226}Ra and (f) Mn. These plots contain all data points over the three-year time series for each depth. Estuarine release of Ba and ^{226}Ra is evident at intermediate salinities in (a) and (c). The sorption edge for ^{226}Ra is apparent at pH 6 in (d). Theoretical barite saturation is shown in (a).

versely related to the groundwater pH, with greater dissolved Ra expected at lower pH (Beck and Cochran, 2013).

To determine whether pH or salinity controlled the dissolved Ra and Ba concentrations over the time series, we examined the relationship between changes in salinity and pH and dissolved Ba and ^{226}Ra across the wide concentration ranges present in the STE. A change is defined as the difference in the parameter (i.e. salinity, pH, ^{226}Ra or Ba) from time point n to time point $n+1$. Thus a positive value indicates an increase in that parameter with time (Fig. 5). According to the K_d dependence described above, we expect an increase in salinity to desorb radium and barium, i.e. a positive relationship between changes in salinity and dissolved concentrations, while an increase in pH will result in sorption, i.e. a negative relationship between pH and changes in dissolved concentrations. We observe a positive trend between changes in salinity and changes in ^{226}Ra and Ba (Fig. 5 and Supplemental Table 1). However, this relationship varies with location in the subterranean estuary. For example, there is a much lower slope between salinity changes and corresponding Ba and ^{226}Ra changes within the region of Mn–Fe oxide coated sediments (5.5 m) compared to sediments above this region, likely due to the high affinity of Mn-oxide coated sediments for Ba and Ra. While we observe the expected negative relationship between changes in pH and dissolved ^{226}Ra and Ba, this relationship is never significant (Fig. 5 and Supplemental Table 1). Further evidence that changes in pH are not associated with sorption and release of Ba and Ra is provided by the lack of Ba and Ra variability at 2.4 m, where the pH range is the most dynamic (5–7), but low salinity is maintained. Given the occurrence of the highest dissolved Ba and Ra within the region of the largest salinity gradients over time (3.1–4.1 m) and the significant positive relationship between changes in salinity and ^{226}Ra (from 3.4 to 4.2 m) and Ba (at 3.4, 4.0 and 5.0 m), we conclude that ion exchange reactions were driving the large seasonal releases of these elements. These adsorption/desorption reactions occur on a timescale of hours such that the dissolved Ra in groundwater is expected to reach equilibrium rapidly with the sediment Ra pool (Gonneea et al., 2008).

The similar behavior of Ba and Ra, which suggests that they had the same source and were driven by similar processes, has been observed previously in the STE (Charette et al., 2005; Gonneea et al., 2008; Kiro et al., 2012). Considering the three orders of magnitude range in Ba and ^{226}Ra concentrations, these elements were well correlated over time and at different depths and groundwater salinities within the STE (all data $r^2 = 0.5$, $p < 0.0001$). Hence, ^{226}Ra was behaving like a stable element, and therefore its cycling did not appear to be controlled by production from its sediment-bound parent ^{230}Th. Modeling results in the Waquoit coastal aquifer further support this conclusion. Michael et al. (2011) determined steady state ^{226}Ra activities as a function of different production and retardation rates along a flow path (i.e. as a function of time) within both the terrestrial and marine groundwater regions of the subterranean estuary. This model was not able to reproduce the spatial variability evident in Waquoit Bay subterranean estuary solely as a function of the groundwater residence time and salinity, likely due subsurface heterogeneity in production/retardation factors and nonsteady-state conditions (Michael et al., 2011). This is in contrast to a similar study of the Dead Sea aquifer, where the groundwater ^{226}Ra activity was explained by mixing between modified Dead Sea water mixing with Ra-poor terrestrial water (Kiro et al., 2012).

We hypothesize that the sediments of the subterranean estuary were acting as a geochemical capacitor for ^{226}Ra and Ba on seasonal time scales as previously proposed for the Ganges–Brahmaputra River Delta by Moore (1997). Q6 During periods of low hydraulic gradient across the STE, landward transgression of the STZ inundated sediments that had previously been bathed in fresh water with high salinity water. This salinity increase led to Ba and ^{226}Ra desorption from sediments as a result of the lower partition coefficient for these elements at high salinity. When the hydraulic gradient increased, the flux of fresh water over these sediments resulted in an increase in sorption, due to both the decrease in salinity (and concurrent increase in the partition coefficient) and the prior removal of Ba and ^{226}Ra from sediment surfaces during periods of high salinity (i.e. there was an increase in the ion exchange capacity).

Please cite this article in press as: Gonneea M. E., et al. Seasonal cycles in radium and barium within a subterranean estuary: Implications for groundwater derived chemical fluxes to surface waters. *Geochim. Cosmochim. Acta* (2013), http://dx.doi.org/10.1016/j.gca.2013.05.034

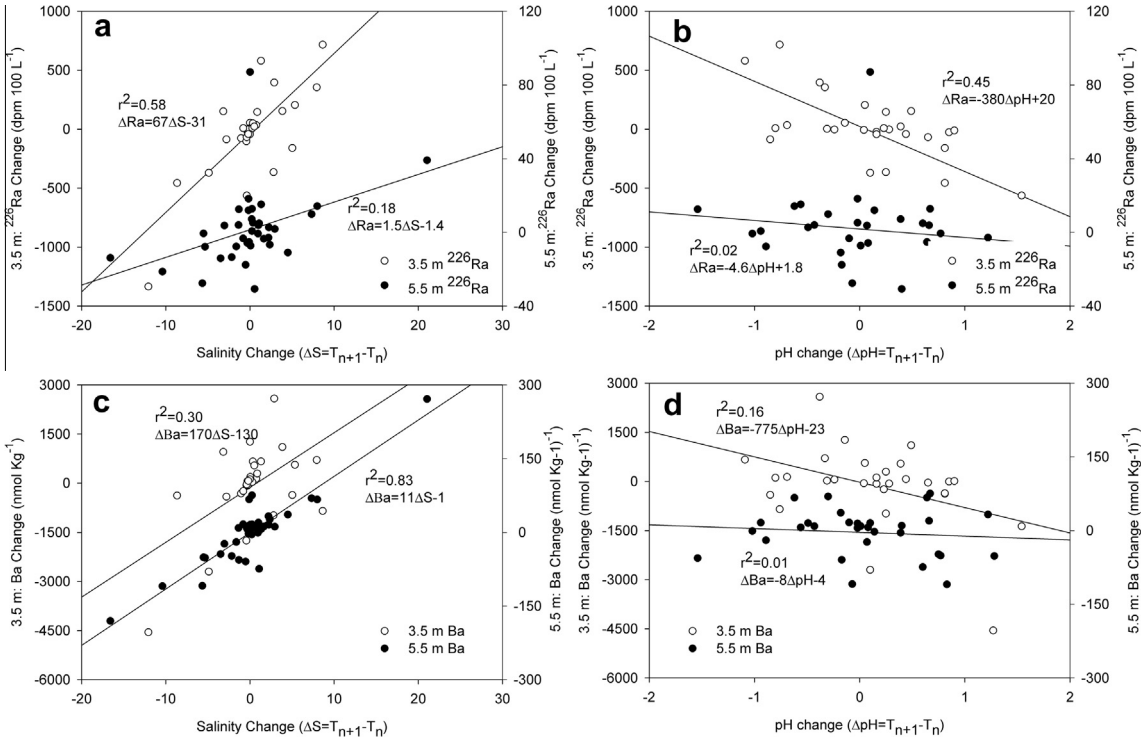

Fig. 5. Temporal changes between groundwater salinity and (a) ^{226}Ra and (c) Ba and pH and (b) ^{226}Ra and (d) Ba during the three-year time series from two depths within the subterranean estuary. The record at 3.5 m was within the region of greatest salinity, pH, Ba and Ra variability, while 5.5 m was within the Mn–Fe oxide region. The change in salinity and pH is defined as ΔS or $\Delta pH = t_{n+1} - t_n$, where t is the time point and n is the number, whereby a positive value indicates the salinity or pH has increased between time points. ΔSalinity is positively correlated with changes in both ^{226}Ra and Ba. The negative relationship between changes in pH and both ^{226}Ra and Ba is poorly correlated. The relationship between ΔS and ^{226}Ra and Ba varies based on location (depth) within the subterranean estuary, indicating a potential control by sediment geochemistry on the sensitivity of the partition coefficient (K_d) to changes in salinity. Note different axes for data from each depth. Supplemental Table 1 includes the relationship and correlation coefficient for these relationships for all depths.

Previous studies of the STE of Waquoit Bay have highlighted the importance of redox cycling of Mn and Fe oxides to alkaline earth elements (such as Ba and Ra) that have an affinity to sorb to these oxide phases (Charette and Sholkovitz, 2006; Dulaiova et al., 2008; Gonneea et al., 2008). While surface bound Ra and Ba on sediments are not directly controlled by groundwater redox conditions, these elements do have an affinity for Mn and Fe oxides and thus were found in the core of the reducing marine groundwater (Spiteri et al., 2006; Gonneea et al., 2008). Our data support the idea that the Mn oxide cycle responded to seasonal oscillations in salinity, as the region with elevated dissolved Mn fluctuated concurrently with salinity (Fig. 2d). The highest concentration of dissolved Mn was found within the region of the subterranean estuary dominated by marine groundwater, at depths greater than 4.5 m for much of the year, and coincided with the region of high sediment bound Mn-oxides. This region of Mn oxides likely helped maintain the relatively constant ^{226}Ra activities found in the saline region of the subterranean estuary due to effective scavenging of ^{226}Ra, as the Mn oxide region has about three times the adsorbed ^{226}Ra compared to sediments in other portions of the STE (Gonneea et al., 2008). Beck and Cochran (2013) suggest that the presence of sediment Mn–Fe oxide coatings effectively buffer dissolved concentrations, as we observe here in the Mn and Fe curtain regions of the subterranean estuary, where dissolved ^{226}Ra and Ba are elevated but temporally stable. However, there is no evidence for Mn oxide dissolution (i.e. high dissolved Mn) in the region between 3.1 and 4.1 m concurrent with the dynamic cycling of Ba and Ra. Thus dissolution and precipitation of Mn oxides do not appear to be driving the large seasonal releases of Ba and Ra. However, it is the presence of Mn–Fe oxides on sediments throughout the subterranean estuary that resulted in increased partitioning between the adsorbed and dissolved phase since sediments coated with oxides have higher K_d's than sediments without these oxides (Gonneea et al., 2008; Beck and Cochran, 2013). Subterranean estuary sediments outside the extremely enriched Fe and Mn curtains have adsorbed Mn of 50–100 μmol kg^{-1} and adsorbed Fe of 3000–8000 μmol kg^{-1}. Indeed, we propose that it is the increase in Fe–Mn oxides on sediments within the STE compared to inland aquifer sediments that is responsible for these sediments sorbing radium and barium from terrestrial groundwater flowing into the subterranean estuary. Recently Beck and Cochran (2013) reported a 4–5-fold increase in Mn and Fe content over eight months in "pristine" sands deposited on a Virginia beach for replenishment, demonstrating that sediment alteration within the coastal subterranean estuary occurs rapidly.

Please cite this article in press as: Gonneea M. E., et al. Seasonal cycles in radium and barium within a subterranean estuary: Implications for groundwater derived chemical fluxes to surface waters. *Geochim. Cosmochim. Acta* (2013), http://dx.doi.org/10.1016/j.gca.2013.05.034

We also considered the importance of barite ($BaSO_4$) formation on scavenging Ra from solution, since this mechanism has been shown to be important in ocean sediments (Paytan et al., 1996), laboratory experiments (Beck and Cochran, 2013) and in the Dead Sea aquifer (Kiro et al., 2012). If such a mechanism were important we would expect removal of dissolved Ba and Ra concurrently with an increase in salinity. In fact, the opposite is observed, with an increase in salinity concurrent with groundwater Ba and Ra concentrations, at times above barite saturation. Ba concentrations that exceed theoretical barite saturation have been observed many times in the subterranean estuary, perhaps due to slow kinetics of barite precipitation or stabilization with organic ligands (Shaw et al., 1998; Windom and Niencheski, 2003; Charette and Sholkovitz, 2006; Santos et al., 2011). Thus, barite formation does not appear to control dissolved Ba and Ra within the time series data presented here. Thus, we do not believe barite formation controls dissolved Ba and Ra within the time series data presented here.

4.2. Potential Ra and Ba fluxes to Waquoit Bay surface waters

We evaluated the influence of temporally changing groundwater end members on SGD-associated fluxes to Waquoit Bay surface waters by combining the results of the hydrodynamic model with the time series chemical data. Given the dynamic character of the salinity transition zone, the end member chemistry of discharging water was expected to be a mixture of water from different regions of the STE, as has been shown previously by Michael et al. (2011). The results from the hydrodynamic model provided both total flux and the salinity of that flux. Thus, we divided the groundwater flux into different pools based on the salinity of the discharging water. To do this, the modeled groundwater discharge was sorted into five different salinity groups (0–5, >5–10, >10–15, >15–20 and >20). Groundwater-derived Ra and Ba fluxes were then calculated by multiplying average groundwater radium and barium concentrations times water fluxes within the same salinity groups. Fluxes were determined for each month from January 2005 through May 2007 (Fig. 6).

Such a salinity-weighted approach to determining groundwater chemical fluxes assumes that the chemistry of the groundwater sampled corresponds to the chemistry of the modeled water flux for each salinity group. Michael et al. (2011) demonstrated that the Ra activity of groundwater was closely tied to the sampling location within the STE. The ^{226}Ra activity reported by Michael et al. (2011) for different regions within the STE tend to correspond to similar salinity groups used in the present study, with the exception of ^{226}Ra activity used for the >20 salinity marine groundwater. In the time series data presented here, ^{226}Ra in the >20 salinity fraction was 41 ± 7.7 dpm 100 L^{-1}, a value much closer to the activity Michael et al. (2011) reported for discharge away from the mixing zone (~23 dpm 100 L^{-1}) than the activity of the deep marine groundwater (~290 dpm 100 L^{-1}) below the mixing zone (Michael et al., 2011). Thus the fluxes presented here associated with the marine groundwater end member may be underestimates if much of the saline discharge originates below the mixing zone.

To calculate the chemical flux of Ra and Ba associated with groundwater discharge, we only considered water discharging across the full mixing zone of the model (the region beginning at the CCC1 well and extending 130 m seaward, see Gonneea et al. (2013) for further details). We did not consider recirculated water being pumped in and out of sediments further out in the bay (i.e. >100 m from mean sea level), which may be a significant flux of recirculated seawater. This water flux was not considered in the present study because it has the same ^{226}Ra activity as bay water (Michael et al., 2011) and thus likely had no net effect on the ^{226}Ra flux associated with groundwater transport through the STE.

There is a strong seasonality in the modeled water flux and salinity of discharging water (Fig. 6). The average shoreline normalized terrestrial groundwater flux was 3.4 ± 0.46 (minimum 2.6, maximum 4.6) $m^3\ m^{-1}\ day^{-1}$ and varied little with time. There was a large temporal variability in discharge of marine groundwater of 1.6 ± 1.4 (minimum 0.39, maximum 4.7) $m^3\ m^{-1}\ day^{-1}$ and associated submarine groundwater recharge (SGR), the inflow of bay water into the STE. Model-derived groundwater fluxes of both terrestrial (salinity of 0) and marine (bay water salinity of 30) fluxes compare well with previously reported estimates. Terrestrial groundwater discharge rates along the head of Waquoit Bay determined from a variety of techniques are reported to be 1.6–1.8 $m^3\ m^{-1}\ day^{-1}$ (recharge method, Cambareri and Eichner (1998)), 3.5 $m^3\ m^{-1}\ day^{-1}$ (seepage meters, Michael (2004)) and 4.0 $m^3\ m^{-1}\ day^{-1}$ (Darcy method, Mulligan and Charette (2006). Marine groundwater discharge estimates are more variable between 0.6 $m^3\ m^{-1}\ day^{-1}$ (radium isotopes, Mulligan and Charette (2006)) and 6.9 $m^3\ m^{-1}\ day^{-1}$ (seepage meters, Michael (2004)).

Groundwater radium activities and barium concentrations were not in phase with the water flux, with maximum concentrations occurring in October 2005, May 2006, December 2006, and July 2007 (Fig. 6). Water fluxes peaked from May to October 2005 and 2006. Since the magnitude of the change in groundwater radium activities and barium concentrations was greater than the relative change in water flux, the amount of radium and barium exported to the bay was dominated by the changes in STE radium activities and barium concentrations. The range in ^{226}Ra and Ba fluxes was 110–5710 dpm $m^{-1}\ d^{-1}$ and 0.1–8.4 mmol $m^{-1}\ d^{-1}$. This ^{226}Ra flux compares well to a previous flux of 1080 dpm $m^{-1}\ d^{-1}$ in July 2003 reported by Mulligan and Charette (2006). Integrating across the 2 y of model and time series data (January 2005 to December 2006), the shoreline normalized radium and barium fluxes were $67–84 \times 10^4$ dpm $m^{-1}\ y^{-1}$ for ^{226}Ra, $160–280 \times 10^4$ dpm $m^{-1}\ y^{-1}$ for ^{228}Ra, $300–430 \times 10^4$ dpm $m^{-1}\ y^{-1}$ for ^{224}Ra, and 0.59–0.70 mol $m^{-1}\ y^{-1}$ for Ba (Table 1).

Potential uncertainty in these chemical flux measurements may stem from either variability in water flux or end member concentration. As discussed above, water fluxes are well within previously reported values, giving us some confidence in this parameter. Uncertainty in end

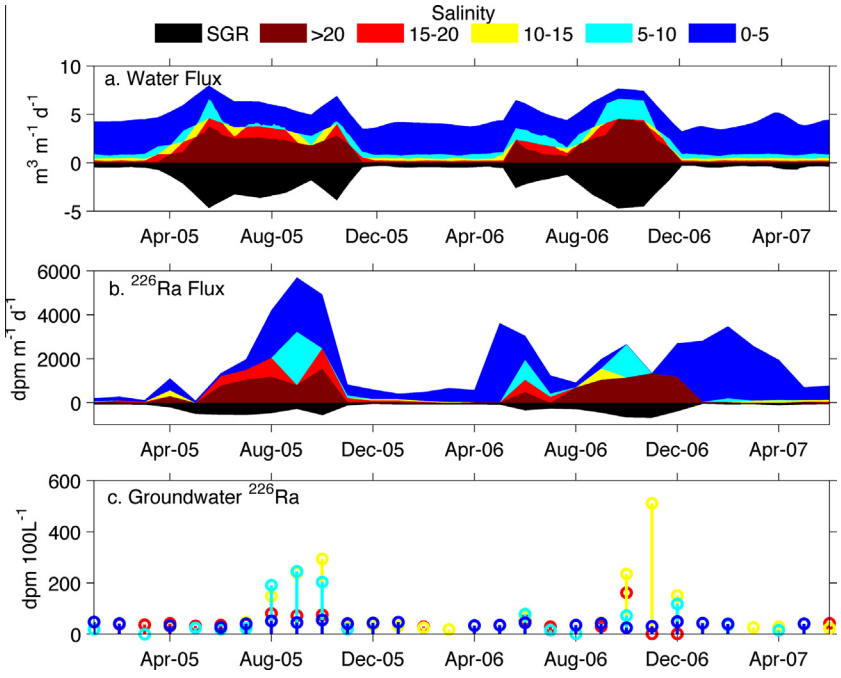

Fig. 6. (a) Model derived submarine groundwater discharge, (b) ^{226}Ra flux calculated with water fluxes from the hydrologic model and (c) contemporaneous ^{226}Ra end member activities. The water and ^{226}Ra fluxes and ^{226}Ra groundwater activities are divided into five different salinity end members. Ra flux is not in phase with water flux throughout much of the record since the groundwater end member variability dominates the radium flux term.

Table 1
Water, Ba and ^{226}Ra budget for the Waquoit Bay subterranean estuary.

	Water flux ($m^3\ m^{-1}\ y^{-1}$)		Ba flux ($mol\ m^{-1}\ y^{-1}$)		^{226}Ra flux ($10^4\ dpm\ m^{-1}\ y^{-1}$)	
	Year 1[a]	Year 2	Year 1	Year 2	Year 1	Year 2
Input to STE						
Terrestrial groundwater[b]	1200	1200	0.15	0.14	18	18
Submarine groundwater recharge (SGR)[c]	730	620	0.05	0.04	11	9.3
Output from the STE						
Submarine groundwater discharge	1930	1820	0.70	0.59	67	84
Excess flux from STE						
(output–input)	–	–	0.50	0.41	38	57
% of input	–	–	250	230	130	210

[a] Hydrologic model year 1/2 driven by 2005/2006 groundwater and sea level records. All fluxes are normalized to per meter of shoreline. To scale fluxes to the entire head of Waquoit Bay for comparison with previous work (i.e. Mulligan and Charette, 2006; Michael et al., 2011), multiply by 610 m.

[b] Terrestrial groundwater end member used was: Ba 120 $nmol\ kg^{-1}$ and ^{226}Ra 15 dpm 100 L^{-1} (Charette and Sholkovitz, 2006; Gonneea et al., 2008).

Q11 [c] Waquoit Bay water (source of recirculating marine groundwater) Ba is 70 $nmol\ kg^{-1}$ and ^{226}Ra 15 dpm 100 L^{-1} (Charette et al., 2001, 2006; Charette, unpublished data).

member concentrations is difficult to determine since Ba and ^{226}Ra concentrations were under sampled—that is there were only eight measurements at each sampling time point. While this approach allows us to account for temporal variability, which we found to be large, we cannot determine the full range of potential Ba and ^{226}Ra values within the STE at each time point. We discuss in the next section how the chosen end members impact our evaluation of the ^{226}Ra and Ba budgets of the subterranean estuary.

4.3. Seasonal budgets of ^{226}Ra and Ba within the subterranean estuary

Since the dynamic temporal scale of the subterranean estuary was seasonal, we expect fluxes into and out of the

system to be equal over the course of a year if the system is at steady state. To determine if the subterranean estuary Ba and ^{226}Ra budgets were in balance during the two complete years with water flux data, we calculated inputs to the STE from both terrestrial groundwater and recharging marine groundwater (Table 1). Input to the STE from terrestrial groundwater was calculated using the fresh water flux from the hydrologic model and terrestrial groundwater end member Ba and ^{226}Ra concentrations. Groundwater flowing into the Waquoit Bay subterranean estuary has a Ba concentration of 60 ± 60 nmol kg^{-1} ($n = 44$, measured across multiple years and seasons) and a ^{226}Ra activity of 11 ± 4 dpm 100 L^{-1} ($n = 14$) (Charette unpublished data; Charette and Sholkovitz, 2006; Gonneea et al., 2008). We used end member concentrations of 120 nmol kg^{-1} Ba and 15 dpm 100 L^{-1} ^{226}Ra to ensure we considered maximum potential fluxes into the STE. The input from submarine groundwater recharge was derived from the bay water Ba and ^{226}Ra end member concentrations and the SGR flux in the hydrologic model (Table 1). Bay water Ba and ^{226}Ra has likewise been measured in multiple seasons and years and is 56 ± 14 nmol kg^{-1} ($n = 68$) and 11 ± 4 dpm 100 L^{-1} ($n = 53$) (Charette unpublished data; Charette et al., 2001; Charette and Sholkovitz, 2006). Again, to ensure maximum fluxes into the STE, we used 70 nmol Ba kg^{-1} and 15 dpm ^{226}Ra 100 L^{-1} as end member concentrations.

This simple model of Ba and ^{226}Ra within the STE suggests that there is an excess flux (i.e. flux out-flux in) out of the subterranean estuary of both Ba and ^{226}Ra equivalent to 130–250% of total inputs (Table 1). Changes in either terrestrial or marine groundwater fluxes are unlikely to balance the input deficit, since any increase in these water fluxes results in a concurrent increase in SGD and associated export of Ba and ^{226}Ra. Weathering and production via decay of ^{230}Th (in the case of ^{226}Ra) are also too small to account for the imbalance. *In situ* production is estimated at only 0.007% of the excess ^{226}Ra flux (44 dpm ^{226}Ra m^{-1} y^{-1}, production ^{226}Ra $= A^{230}$Th $\times \lambda^{226}$Ra/K_d, with an estimated ^{230}Th of 400 dpm kg^{-1} and K_d of 1000; 130 m wide interface, 10 m deep). The Ba flux from weathering is approximately 0.05% of the excess Ba flux (2.9×10^{-4} mol m^{-1} y^{-1}, calculated from an average grain size of 550 microns and Ba weathering rate of 2.7×10^{-10} mol m^{-2} y^{-1} (Bowen, 1979; White, 2003)).

Alternatively, the terrestrial groundwater and/or the bay water Ba and ^{226}Ra end members used in this budget may be too low. Michael et al. (2011) predicted equilibrium values for ^{226}Ra within the fresh portion of the STE to be 30 dpm 100 L^{-1}, which is twice our average value, but would still result in ^{226}Ra inputs to the STE equaling only of 54–70% of total ^{226}Ra export via SGD. The SGR input of Ba and ^{226}Ra was only 22–38% of total inputs, thus the bay end member values would need to be much larger to bring the Ba and ^{226}Ra budget into balance. The budget as calculated here already uses end members at the high end of previously measured values, thus inputs to the subterranean estuary are unlikely to be larger.

This large groundwater Ba and ^{226}Ra flux imbalance may result from a net sea level rise over the sampling time period, since sea level appears to be the main control of the movement of the salinity mixing zone (Gonneea et al., 2013). Sea level rise would result in sediments with large adsorbed pools of Ra and Ba being inundated repeatedly with marine groundwater, thereby releasing these elements into solution as hypothesized previously by Shaw et al. (1998). Indeed, mean sea level rise was 0.5 cm y^{-1} from 1990 to 2007, with a large step-wise increase in mean sea level of 5 cm between the periods of 2000–2004 and 2005–2006, the duration of this study (NOAA, 2012). The northeast coast of the United States is experiencing accelerating sea level rise, accounting for the observed dynamic sea level during this study (Sallenger et al., 2012). It is apparent that in addition to yearly seasonal oscillations in ^{226}Ra and Ba flux there are additional releases of these chemically reactive materials. During the preceding lower sea level stands, these elements were stored in the STE and are currently being released and exported via SGD.

We can compare the excess flux to the desorbable sediment pool of ^{226}Ra and Ba in the STE. Given the above mentioned sea level rise (5 cm) just prior to beginning our field sampling, approximately 6.5 m^3 of aquifer per meter of shoreline was newly inundated across our model domain (130 m). The desorbable ^{226}Ra pool in that volume of aquifer (calculated from 100 dpm kg^{-1} dry sediment, 2.6 g cm^{-1} sediment density and 0.25 sediment porosity, Gonneea et al., 2008) is 126×10^4 dpm, 3–4 times greater than observed excess fluxes. Likewise, the desorbable pool of Ba (110 μmol kg^{-1} dry sediment, Charette, unpublished data) present in the same aquifer volume is 1.41 mol, about 2 times greater than the observed excess fluxes. Therefore, the observed sea-level rise could account all of the excess ^{226}Ra and Ba flux observed in this study.

Our knowledge of sediment geochemistry both in the subterranean estuary and beyond is limited. Sorbed ^{226}Ra at one location within the Mn-curtain of Waquoit Bay reached 320 dpm kg^{-1}, while sorbed Ba of 300–400 μmol kg^{-1} has been observed on coastal and inland sediments (Gonneea et al., 2008; Charette, unpublished data). It is possible that the sediment pools of ^{226}Ra and Ba are larger than calculated here and thus accelerating sea level rise may result in greater export of ion exchangeable elements such as these. This finding highlights that there may be a potential increase in chemical flux via submarine groundwater discharge as sea level rises in concert with predicted climate change.

5. CONCLUSIONS

Radium fluxes to surface waters at the head of Waquoit Bay are a function of two parameters, the volume flux of water and the end member radium activity of that water. In the time series data presented here, temporal variability in radium concentrations was much greater than the corresponding change in water flux. As a result, radium fluxes were at times anti-phased with water fluxes. This conclusion highlights the importance of determining a groundwater end member radium concentration contemporaneously with any radium tracer calculation of submarine groundwater discharge. An increased flux of radium cannot *a priori* be assumed to indicate an increase in submarine groundwa-

Please cite this article in press as: Gonneea M. E., et al. Seasonal cycles in radium and barium within a subterranean estuary: Implications for groundwater derived chemical fluxes to surface waters. *Geochim. Cosmochim. Acta* (2013), http://dx.doi.org/10.1016/j.gca.2013.05.034

ter discharge without understanding how radium cycling within the subterranean estuary affects the radium activity of the discharging water.

This temporal disconnect between water and radium fluxes has important implications for studies that utilize radium tracer budgets to determine seasonal variability in SGD. Recently Moore and Shaw (2008) observed an increased radium flux during the summer months in coastal estuaries off the U.S. Atlantic coast and attributed this to an increase in SGD due to increased marsh interactions (i.e. bioirrigation) in the summer time and to a lag between precipitation and SGD. Kelly and Moran (2002) measured seasonally variable radium fluxes to the Pettaquamscutt Estuary, Rhode Island, and observed the highest fluxes of radium in the summer. Groundwater radium values for this study were measured once (in August) and used to calculate SGD values, which they concluded were higher in the summer than the winter, in phase with the radium flux. A recent study in this same region collected groundwater during different seasons and recognized that variability in the pore water activity likely accounted for some of the increased radium flux observed (Hougham et al., 2008). Increases in radium fluxes, such as reported here and in the works listed above, may not be due solely to an increase in submarine groundwater discharge, but also to an increase in the end member radium activity. Thus these findings highlight the importance of understanding the background hydrology of the system under study when applying radium tracers of SGD. Furthermore, the assumption of temporally constant radium activities is clearly invalid in the face of significant temporal salinity changes within the subterranean estuary. Additional time series measurements of groundwater chemistry in other subterranean estuaries would confirm the role seasonal cycling plays in groundwater radium and barium concentrations within coastal aquifer systems.

Temporal variability in groundwater radium and barium concentrations ranged over three orders of magnitude during a three-year time series of the subterranean estuary of Waquoit Bay. These fluctuations resulted from movement of the salinity interface resulting in a narrow region (approximately 1 m vertical extent) that experiences large fluctuations in water chemistry (Gonneea et al., 2013). Concurrent with an increase in salinity within this dynamic region are large releases of the alkaline earth elements Ba and Ra, suggesting that ion exchange reactions are the most important process controlling seasonal variability and that the subterranean estuary acts as an ion exchange reservoir for these elements on seasonal time scales. Ra and Ba are added to terrestrial groundwater upland of the subterranean estuary and are then transported to the salinity-mixing zone of the subterranean estuary. Here Ba and Ra are concentrated onto sediments at the coast due to Mn–Fe oxides coatings, and then are released or sorbed due to changes in groundwater salinity.

The behavior of the subterranean estuary as an "ion capacitor" has important implications for the timing of the release of chemically reactive constituents via submarine groundwater discharge. For example, SGD-derived fluxes of contaminants to surface waters involved in salinity or redox driven reactions could be modulated in a similar way (e.g. mercury (Bone et al., 2007) and arsenic (Bone et al., 2006; Jung et al., 2009)). These processes may also result in the uncoupled transport of anions and cations, as has been observed for nitrate and phosphate (de Sieyes et al., 2008; Slomp and Van Cappellen, 2004).

On the time scale of this study, export of Ba and Ra from the subterranean estuary cannot be balanced with respect to known imports. We contend that this is a result of long term storage of these cations within the sediments of the STE as has been hypothesized elsewhere (Moore and Shaw, 1998; Shaw et al., 1998) and subsequent release during the current period of accelerating sea level rise (Yin et al., 2009; Sallenger et al., 2012). Super imposed upon seasonal oscillations in groundwater chemistry in sync with sea level fluctuations are other perturbations in sea level, caused by wind and ocean circulation changes coincident with El Niño and North Atlantic Oscillation (NAO) dynamics (Llovel et al., 2011; Sweet and Zervas, 2011). Interannual climate fluctuations that control sea level and precipitation (e.g. ENSO and NAO), and thus the position of the mixing zone within the subterranean estuary, may ultimately control the timing and magnitude of chemical and water flux via submarine groundwater discharge. Our results may also require a reevaluation of any trace element mass balance models (e.g. Sr (Basu et al., 2001; Beck et al., in press) and U (Dunk et al., 2002)) for the ocean that rely on a steady-state contribution from terrestrial sources such as SGD.

ACKNOWLEDGEMENTS

The authors thank Paul Henderson, Gillian Smith, DeAnna McCadney and Grace Rago for assistance in the field and laboratory. Scot Birdwhistell of the WHOI ICP-MS Facility assisted with trace metal analyses. We extend our continued appreciation to the director and staff of the Waquoit Bay National Estuarine Research Reserve for their assistance with logistics during field sampling. Comments by Associate Editor Tim Shaw and two anonymous reviewers greatly improved this work. This research was sponsored by NSF (OCE-0425061 to M.A.C. and A.E.M. and OCE-0751525 to M.A.C.). M.E.G. was supported by an NDSEG graduate fellowship and was awarded a graduate fellowship from the Estuarine Reserves Division, Office of Ocean and Coastal Resource Management, National Ocean Service, National Oceanic and Atmospheric Administration.

APPENDIX A. SUPPLEMENTARY DATA

Supplementary data associated with this article can be found, in the online version, at http://dx.doi.org/10.1016/j.gca.2013.05.034.

REFERENCES

Abarca E., Karam H. N., Hemond H. F. and Harvey C. F. (2013) Transient groundwater dynamics in a coastal aquifer: the effects of tides, the lunar cycle and the beach profile. *Water Resour. Res.*. http://dx.doi.org/10.1002/wrcr.20075.

Basu A. R., Jacobsen S. B., Poreda R. J., Dowling C. B. and Aggarwal P. K. (2001) Large groundwater strontium flux to the

oceans from the Bengal basin and the marine strontium isotope record. *Science* **293**, 1470–1473.

Beck A. J., Charette M. A., Cochran J. K., Gonneea M. E. and Peucker-Ehrenbrink B. (2013) Dissolved strontium behavior in the subterranean estuary – implications for the Sr isotope budget of the global ocean. *Geochim. Cosmochim. Acta*, in press.

Beck A. J., Cochran J. K. and Sanudo-Wilhelmy S. A. (2010) The distribution and speciation of dissolved trace metals in a shallow subterranean estuary. *Mar. Chem.* **121**, 145–156.

Beck A. J. and Cochran M. A. (2013) Controls on solid-solution partitioning of radium in saturated marine sands. *Mar. Chem.*, http://dx.doi.org/10.1016/j.marchem.2013.01.008.

Beck A. J., Tsukamoto Y., Tovar-Sanchez A., Huerta-Diaz M., Bokuniewicz H. J. and Sanudo-Wilhelmy S. A. (2007) Importance of geochemical transformations in determining submarine groundwater discharge-derived trace metal and nutrient fluxes. *Appl. Geochem.* **22**, 477–490.

Bone S. E., Charette M. A., Lamborg C. H. and Gonneea M. E. (2007) Has submarine groundwater discharge been overlooked as a source of mercury to coastal waters? *Environ. Sci. Technol.* **41**, 3090–3095.

Bone S. E., Gonneea M. E. and Charette M. A. (2006) Geochemical cycling of arsenic in a coastal aquifer. *Environ. Sci. Technol.* **40**, 3273–3278.

Bowen H. J. M. (1979) *Environmental Chemistry of the Elements*. Academic Press, London, UK and New York, NY, USA.

Breier J. A., Breier C. F. and Edmonds H. N. (2010) Seasonal dynamics of dissolved Ra isotopes in the semi-arid bays of south Texas. *Mar. Chem.* **122**, 39–50.

Cambareri T. C. and Eichner E. M. (1998) Watershed delineation and ground water discharge to a coastal embayment. *Ground Water* **36**, 626–634.

Charette M. A. (2007) Hydrologic forcing of submarine groundwater discharge: insight from a seasonal study of radium isotopes in a groundwater-dominated salt marsh estuary. *Limnol. Oceanogr.* **52**, 230–239.

Charette M. A. and Allen M. C. (2006) Precision ground water sampling in coastal aquifers using a direct-push, shielded-screen well-point system. *Ground Water Monit. Remediat.* **26**, 87–93.

Charette M. A., Buesseler K. O. and Andrews J. E. (2001) Utility of radium isotopes for evaluating the input and transport of groundwater-derived nitrogen to a Cape Cod estuary. *Limnol. Oceanogr.* **46**, 465–470.

Charette M. A. and Sholkovitz E. R. (2006) Trace element cycling in a subterranean estuary: Part 2. Geochemistry of the pore water. *Geochim. Cosmochim. Acta* **70**, 811–826.

Charette M. A., Sholkovitz E. R. and Hansel C. M. (2005) Trace element cycling in a subterranean estuary: Part 1. Geochemistry of the permeable sediments. *Geochim. Cosmochim. Acta* **69**, 2095–2109.

De Geer L.-E. (2004) Currie detection limits in gamma-ray spectroscopy. *Appl. Radiat. Isotopes* **61**, 151–160.

Dulaiova H., Gonneea M. E., Henderson P. B. and Charette M. A. (2008) Geochemical and physical sources of radon variation in a subterranean estuary – implications for groundwater radon activities in submarine groundwater discharge studies. *Mar. Chem.* **110**, 120–127.

Dunk R. M., Mills R. A. and Jenkins W. J. (2002) A reevaluation of the oceanic uranium budget for the Holocene. *Chem. Geol.* **190**, 45–67.

Elsinger R. J. and Moore W. S. (1980) Ra-226 behavior in the Pee-Dee River Winyah Bay Estuary. *Earth Planet. Sci. Lett.* **48**, 239–249.

Ferrarin C., Rapaglia J., Zaggia L., Umgiesser G. and Zuppi G. M. (2008) Coincident application of a mass balance of radium and a hydrodynamic model for the seasonal quantification of groundwater flux into the Venice Lagoon, Italy. *Mar. Chem.* **112**, 179–188.

Gonneea M. E., Morris P. J., Dulaiova H. and Charette M. A. (2008) New perspectives on radium behavior within a subterranean estuary. *Mar. Chem.* **109**, 250–267.

Gonneea M. E., Mulligan A. and Charette M. A. (2013) Climate-driven sea level anomalies modulate coastal groundwater dynamics and discharge. *Geophys. Res. Lett.*

Hall G. E. M., Vaive J. E., Beer R. and Hoashi M. (1996) Selective leaches revisited, with emphasis on the amorphous Fe oxyhydroxide phase extraction. *J. Geochem. Explor.* **56**, 59–78.

Hougham A. L., Moran S. B., Masterson J. P. and Kelly R. P. (2008) Seasonal changes in submarine groundwater discharge to coastal salt ponds estimated using Ra-226 and Ra-228 as tracers. *Mar. Chem.* **109**, 268–278.

Jung H. B., Charette M. A. and Zheng Y. (2009) Field, laboratory, and modeling study of reactive transport of groundwater arsenic in a coastal aquifer. *Environ. Sci. Technol.* **43**, 5333–5338.

Kelly R. P. and Moran S. B. (2002) Seasonal changes in groundwater input to a well-mixed estuary estimated using radium isotopes and implications for coastal nutrient budgets. *Limnol. Oceanogr.* **47**, 1796–1807.

Kiro Y., Yechieli Y., Voss C. I., Starinsky A. and Weinstein Y. (2012) Modeling radium distribution in coastal aquifers during sea level changes: the Dead Sea case. *Geochim. Cosmochim. Acta* **88**, 237–254.

Koulouris G. (1996) Sorption and distribution of 226-Ra in an electrolytic manganeses dioxide column in the presence of other ions. *J. Radioanal. Nucl. Chem.* **212**, 131–141.

Krest J. M. and Harvey J. W. (2003) Using natural distributions of short-lived radium isotopes to quantify groundwater discharge and recharge. *Limnol. Oceanogr.* **48**, 290–298.

Ku T. L., Luo S., Goldstein S. J., Murrell M. T., Chu W. L. and Dobson P. F. (2009) Modeling non-steady state radioisotope transport in the vadose zone – a case study using uranium isotopes at Pena Blanca, Mexico. *Geochim. Cosmochim. Acta* **73**, 6052–6064.

Li X. Y., Hu B. X., Burnett W. C., Santos I. R. and Chanton J. P. (2009) Submarine ground water discharge driven by tidal pumping in a heterogeneous aquifer. *Ground Water* **47**, 558–568.

Llovel W., Meyssignac B. and Cazenave A. (2011) Steric sea level variations over 2004–2010 as a function of region and depth: inference on the mass component variability in the North Atlantic Ocean. *Geophys. Res. Lett.* **38**.

Michael H. A. (2004) *Seasonal Dynamics in Coastal Aquifers: Investigations of Submarine Groundwater Discharge Through Field Measurements and Numerical Models*. Massachusetts Institute of Technology.

Michael H. A., Charette M. A. and Harvey C. F. (2011) Patterns and variability of groundwater flow and radium activity at the coast: a case study from Waquoit Bay, Massachusetts. *Mar. Chem.* **127**, 100–114.

Michael H. A., Mulligan A. E. and Harvey C. F. (2005) Seasonal oscillations in water exchange between aquifers and the coastal ocean. *Nature* **436**, 1145–1148.

Moore W. S. (1997) High fluxes of radium and barium from the mouth of the Ganges–Brahmaputra river during low river discharge suggest a large groundwater source. *Earth Planet. Sci. Lett.* **150**, 141–150.

Moore W. S. (1999) The subterranean estuary: a reaction zone of ground water and sea water. *Mar. Chem.* **65**, 111–125.

Please cite this article in press as: Gonneea M. E., et al. Seasonal cycles in radium and barium within a subterranean estuary: Implications for groundwater derived chemical fluxes to surface waters. *Geochim. Cosmochim. Acta* (2013), http://dx.doi.org/10.1016/j.gca.2013.05.034

Moore W. S. (2003) Sources and fluxes of submarine groundwater discharge delineated by radium isotopes. *Biogeochemistry* **66**, 75–93.

Moore W. S. and Arnold R. (1996) Measurement of Ra-223 and Ra-224 in coastal waters using a delayed coincidence counter. *J. Geophys. Res. Oceans* **101**, 1321–1329.

Moore W. S. and Reid D. F. (1973) Extraction of radium from natural waters using manganese-impregnated acrylic fibers. *J. Geophys. Res.* **78**, 8880–8886.

Moore W. S., Sarmiento J. L. and Key R. M. (2008) Submarine groundwater discharge revealed by Ra-228 distribution in the upper Atlantic Ocean. *Nat. Geosci.* **1**, 309–311.

Moore W. S. and Shaw T. J. (1998) Chemical signals from submarine fluid advection onto the continental shelf. *J. Geophys. Res. Oceans* **103**, 21543–21552.

Mulligan A. E. and Charette M. A. (2009) Groundwater flow to the coastal ocean. In *Encyclopedia of Ocean Sciences* (eds. H. S. John, K. T. Karl and A. T. Steve). Academic Press, Oxford, pp. 88–97.

Mulligan A. E., Langevin C. and Post V. E. A. (2011) Tidal boundary conditions in SEAWAT. *Ground Water* **49**, 866–879.

NOAA (2012) NOAA Tidal Data: Woods Hole Station 8447930. Available from: http://tidesandcurrents.noaa.gov/station_info.shtml?stn=8449130%20Nantucket%20Island,%20MA (accessed on October 1, 2012).

Paytan A., Moore W. S. and Kastner M. (1996) Sedimentation rate as determined by Ra-226 activity in marine barite. *Geochim. Cosmochim. Acta* **60**, 4313–4319.

Paytan A., Shellenbarger G. G., Street J. H., Gonneea M. E., Davis K., Young M. B. and Moore W. S. (2006) Submarine groundwater discharge: an important source of new inorganic nitrogen to coral reef ecosystems. *Limnol. Oceanogr.* **51**, 343–348.

Perry E., Paytan A., Pedersen B. and Velazquez-Oliman G. (2009) Groundwater geochemistry of the Yucatan Peninsula, Mexico: constraints on stratigraphy and hydrogeology. *J. Hydrol.* **367**, 27–40.

Porcelli D. (2008) Investigating groundwater processes using U- and Th-series nuclides. In *Radioactivity in the Environment* (eds. S. Krishnaswami and J. K. Cochran). Elsevier, pp. 105–153 (Chapter 4).

Rama and Moore W. S. (1996) Using the radium quartet for evaluating groundwater input and water exchange in salt marshes. *Geochim. Cosmochim. Acta* **60**, 4645–4652.

Robinson C., Gibbes B. and Li L. (2006) Driving mechanisms for groundwater flow and salt transport in a subterranean estuary. *Geophys. Res. Lett.*. http://dx.doi.org/10.1029/2005gl025247.

Sallenger A. H., Doran K. S. and Howd P. A. (2012) Hotspot of accelerated sea-level rise on the Atlantic coast of North America. *Nature Clim. Change* **2**, 884–888.

Santos I. R., Burnett W. C., Misra S., Suryaputra I. G. N. A., Chanton J. P., Dittmar T., Peterson R. N. and Swarzenski P. W. (2011) Uranium and barium cycling in a salt wedge subterranean estuary: the influence of tidal pumping. *Chem. Geol.* **287**, 114–123.

Shaw T. J., Moore W. S., Kloepfer J. and Sochaski M. A. (1998) The flux of barium to the coastal waters of the southeastern USA: the importance of submarine groundwater discharge. *Geochim. Cosmochim. Acta* **62**, 3047–3054.

Spiteri C., Regnier P., Slomp C. P. and Charette M. A. (2006) pH-Dependent iron oxide precipitation in a subterranean estuary. *J. Geochem. Explor.* **88**, 399–403.

Sun Y. and Torgersen T. (1998) Rapid and precise measurement method for adsorbed Ra-224 on sediments. *Mar. Chem.* **61**, 163–171.

Sweet W. V. and Zervas C. (2011) Cool-season sea level anomalies and storm surges along the U.S. East Coast: climatology and comparison with the 2009/10 El Nino. *Mon. Weather Rev.* **139**, 2290–2299.

Tricca A., Wasserburg G. J., Porcelli D. and Baskaran M. (2001) The transport of U- and Th-series nuclides in a sandy unconfined aquifer. *Geochim. Cosmochim. Acta* **65**, 1187–1210.

Webster I. T., Hancock G. J. and Murray A. S. (1995) Modeling the effect of salinity on radium desorption from sediments. *Geochim. Cosmochim. Acta* **59**, 2469–2476.

White A. F. (2003) Natural weathering rates of silicate minerals. In *Treatise on Geochemistry* (eds. D. H. Heinrich and K. T. Karl). Pergamon, Oxford, pp. 133–168.

Windom H. and Niencheski F. (2003) Biogeochemical processes in a freshwater–seawater mixing zone in permeable sediments along the coast of Southern Brazil. *Mar. Chem.* **83**, 121–130.

Windom H. L., Moore W. S., Niencheski L. F. H. and Jahrike R. A. (2006) Submarine groundwater discharge: a large, previously unrecognized source of dissolved iron to the South Atlantic Ocean. *Mar. Chem.* **102**, 252–266.

Xin P., Robinson C., Li L., Barry D. A. and Bakhtyar R. (2010) Effects of wave forcing on a subterranean estuary. *Water Resour. Res.* **46**.

Yin J. J., Schlesinger M. E. and Stouffer R. J. (2009) Model projections of rapid sea-level rise on the northeast coast of the United States. *Nat. Geosci.* **2**, 262–266.

Associate editor: Timothy J. Shaw\